A Novel 1D Trifocal Tensor-Based Control for Differential-Drive Robots

H. M. Becerra and C. Sagues

***Abstract*— This paper presents an image-based approach to perform visual control for differential-drive robots. We use for the first time the elements of the 1D trifocal tensor directly in the control law. The visual control utilizes the usual teach-by showing strategy without requiring any a prior knowledge of the scene and does not need any auxiliary image. The main contribution of the paper is that the proposed two-steps control law ensures total correction of both position and orientation without switching to any other visual constraint rather than the 1D trifocal tensor. The paper exploits the sliding mode control technique in a square system, ensuring stability and robustness for the closed loop. The good performance of the control system is proven via simulations.**

I. INTRODUCTION

An interesting research field is concerned about visual servoing for mobile robots, which can allow them to improve their navigation capabilities in a single robot task or in cooperative tasks. A way to face the problem of extracting information from images is by using a geometric constraint relating features from such images. Nowadays, two geometric constraints have been well exploited to control mobile robots, epipolar geometry and the homography model. Some examples of epipolar visual control are [1], [2], [3] and [4]. The homography model has been used in several works, for instance [5], [6]. However, these geometric constraints have both serious drawbacks. Epipolar geometry is ill-conditioned with short baseline and with planar scenes. The homography model is not well defined if there is no dominant planes in the scene or with large baselines.

In order to overcome the drawbacks of the typical geometric constraints, we propose a novel approach based on the 1D trifocal tensor. This tensor completely describes the relative geometry of three views and it is independent of the observed scene [7]. The effectiveness of applying the trifocal tensor to recover location information has been proved in [8] and [9]. The first work uses conventional cameras and artificial landmarks on a plane while the second one uses both conventional and omnidirectional cameras. Both of these works propose the trifocal tensor to be used for initialization of bearing-only SLAM algorithms. A recent work [10] presents a visual control for mobile robots based on the elements of a 2D trifocal tensor constrained to a planar motion. This work shows good performance reaching the target location, however the stability properties of the controller are not very clear.

This work was supported by projects DPI 2006-07928, IST-1-045062-URUS-STP and grants of Banco Santander-Univ. Zaragoza and Conacyt-México.

H.M. Becerra and C. Sagues are with DIIS-I3A, University of Zaragoza C/ María de Luna 1, E-50018 Zaragoza, Spain {hector.becerra, csagues}@unizar.es

We propose in this paper an image-based approach to perform visual servoing for differential-drive robots. The visual control is performed using the value of the elements of the 1D trifocal tensor directly in the control law. The approach utilizes the usual teach-by showing strategy without requiring any a prior knowledge of the scene and does not need any auxiliary image. We propose a two-steps control law, the first step performs position correction and the second one corrects orientation. In the first step a tracking problem is solved by using sliding mode control. This controller is designed using the well known methodology for a square system, which allows to develop a clear stability proof for the closed loop system. Once position correction has been reached, we use a single element of the tensor to perform orientation correction. Our approach ensures total correction of the robot location even for initial locations where epipolar geometry or homography based approaches fail.

The paper is organized as follows. Section II specifies the mathematical modeling of the camera, the mobile robot and the geometric constraint. Section III details the design procedure for the control law. Section IV presents the stability analysis. Section V shows the performance of the closed-loop control system via simulations and finally, Section VI provides the conclusions.

II. MATHEMATICAL MODELING

A. Camera Model

We consider the internal camera calibration matrix as follows

$$\mathbf{K} = \begin{bmatrix} \alpha_x & s & x_0 \\ 0 & \alpha_y & y_0 \\ 0 & 0 & 1 \end{bmatrix} \tag{1}$$

where α_x and α_y represent the focal length of the camera in terms of pixel dimensions in the x and y direction respectively, s is the skew parameter and $(x_0,\, y_0)$ are the coordinates of the principal point. We have that $\alpha_x = fm_x$ and $\alpha_y = fm_y$, where f is the focal length in distance units and m_x, m_y are the pixels per distance unit. We assume that the principal point is in the center of the image $(x_0 = 0,$ $y_0 = 0)$ and there is no skew $(s = 0)$. If we denote the extrinsic parameters by $\mathbf{C}$, an image is denoted by $I\,(\mathbf{K}, \mathbf{C})$.

B. Robot Modeling

This work focuses on controlling a differential-drive robot, whose kinematic model can be expressed in state space as follows

$$\begin{bmatrix} \dot{x} \\ \dot{z} \\ \dot{\phi} \end{bmatrix} = \begin{bmatrix} -\sin\phi & 0 \\ \cos\phi & 0 \\ 0 & 1 \end{bmatrix} \begin{bmatrix} \upsilon \\ \omega \end{bmatrix}. \quad (2)$$

Thus, $\mathbf{x} = (x, z, \phi)^T$ represents the state of the robot system, where x and z are the coordinates of the robot position in the plane, ϕ is the robot orientation, expressed as the angle between the robot body-fixed z-axis and the world z-axis, and υ and ω are the translational and angular input velocities, respectively. υ is in the direction of the robot body-fixed z-axis and ω is about the robot y-axis, i.e. rotation in the plane. From now on, we use the notation $s\beta = \sin\beta$, $c\beta = \cos\beta$.

C. The 1D Trifocal Tensor

The trifocal tensor relates geometrically three views. It only depends on the relative locations of the observed scene in the three views. Let us define a global reference system as depicted in Fig. 1(a) with the origin in the third camera. Then, the camera locations with respect to that global reference are $\mathbf{C}_1 = (x_1, z_1, \phi_1)$, $\mathbf{C}_2 = (x_2, z_2, \phi_2)$ and $\mathbf{C}_3 = (x_3, z_3, \phi_3) = (0, 0, 0)$. We assume that the motion is constrained to be planar. The relative locations between cameras is defined by a local reference frame in each camera as is shown in Fig. 1(b).

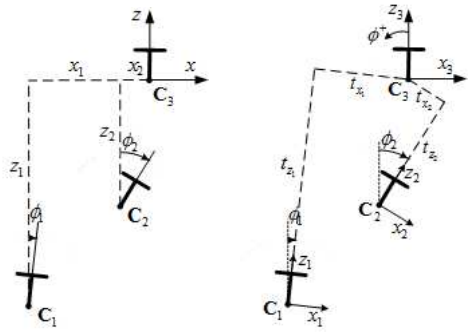

(a) (b)

Fig. 1. (a) Global reference definition, (b) Relative location between cameras.

The expression of the tensor as it is obtained from metric information of the three views is

$$\begin{aligned} \mathbf{T}_1 &= \begin{bmatrix} T_{111} & T_{112} \\ T_{121} & T_{122} \end{bmatrix} \quad (3) \\ &= \begin{bmatrix} t_{z_1}s\phi_2 - t_{z_2}s\phi_1 & -t_{z_1}c\phi_2 + t_{z_2}c\phi_1 \\ t_{z_1}c\phi_2 + t_{x_2}s\phi_1 & t_{z_1}s\phi_2 - t_{x_2}c\phi_1 \end{bmatrix}, \\ \mathbf{T}_2 &= \begin{bmatrix} T_{211} & T_{212} \\ T_{221} & T_{222} \end{bmatrix} \\ &= \begin{bmatrix} -t_{x_1}s\phi_2 - t_{z_2}c\phi_1 & t_{x_1}c\phi_2 - t_{z_2}s\phi_1 \\ -t_{x_1}c\phi_2 + t_{x_2}c\phi_1 & -t_{x_1}s\phi_2 + t_{x_2}s\phi_1 \end{bmatrix} \end{aligned}$$

where $t_{x_i} = -x_i c\phi_i - z_i s\phi_i$, $t_{z_i} = x_i s\phi_i - z_i c\phi_i$ for $i = 1, 2$.

D. Values of the Trifocal Tensor in Particular Locations

We consider camera two ($\mathbf{C}_2$) as the one that moves, however, similar overall results can be obtained considering $\mathbf{C}_1$ as the moving camera. When location of camera $\mathbf{C}_2 = \mathbf{C}_1$, this is $(x_2, z_2, \phi_2) = (x_1, z_1, \phi_1)$, the relative location between these cameras is $t_{x_2} = t_{x_1}$, $t_{z_2} = t_{z_1}$, and the values of the tensor elements produce the following relationships

$$\begin{aligned} T_{111} &= 0,\ T_{112} = 0,\ T_{121} + T_{211} = 0, \quad (4) \\ T_{221} &= 0,\ T_{222} = 0,\ T_{122} + T_{212} = 0. \end{aligned}$$

When locations $\mathbf{C}_2 = \mathbf{C}_3$, this is $(x_2, z_2, \phi_2) = (0, 0, 0)$, the relative location between these cameras is $t_{x2} = 0$, $t_{z2} = 0$, and it gives the following relationships

$$\begin{aligned} T_{111} &= 0,\ T_{122} = 0,\ T_{112} + T_{121} = 0, \quad (5) \\ T_{211} &= 0,\ T_{222} = 0,\ T_{212} + T_{221} = 0. \end{aligned}$$

In order to design a controller to drive the robot to a target location, we have to consider the corresponding final tensor values as a control objective. Also, we have to take into account that the control cannot be initiated with no information from the tensor.

E. Dynamical system from the 1D trifocal tensor

This dynamical system involves the robot model and relates the change of the tensor elements given by a change in the velocities of the robot. It is obtained getting the derivatives of the tensor elements in (3). In practice, the trifocal tensor has an unknown scale factor and it varies as the robot moves. To define a common scale during the navigation, each element of the tensor is divided by a normalizing factor as follows

$$T_{ijk} = \frac{T^m_{ijk}}{T^m_N} \quad (6)$$

where T^m_{ijk} are the trifocal tensor elements computed from metric information of the camera locations, T_{ijk} are the normalized elements and T^m_N is a suitable normalizing factor also computed from metric values. Then, the normalized dynamical system is the following

$$\begin{aligned} \dot{T}_{111} &= \tfrac{s\phi_1}{T^m_N}\upsilon + T_{121}\omega, \quad (7) \\ \dot{T}_{112} &= -\tfrac{c\phi_1}{T^m_N}\upsilon + T_{122}\omega, \\ \dot{T}_{121} &= -T_{111}\omega, \\ \dot{T}_{122} &= -T_{112}\omega, \\ \dot{T}_{211} &= \tfrac{c\phi_1}{T^m_N}\upsilon + T_{221}\omega, \\ \dot{T}_{212} &= \tfrac{s\phi_1}{T^m_N}\upsilon + T_{222}\omega, \\ \dot{T}_{221} &= -T_{211}\omega, \\ \dot{T}_{222} &= -T_{212}\omega. \end{aligned}$$

It is worth noting that the normalizing factor can be seen as a gain for the translational velocity input (υ) and therefore, the normalization may be substituted by a suited gain in the υ input channel. It allows to avoid the problem of having $T^m_N = 0$ if the normalizing factor is not well chosen. In (7) there are four elements that do not depend on υ. It means that a change in υ does not produce a variation in these tensor elements and consequently, only orientation correction can be performed using such elements.

F. Selecting suited outputs

The problem of taking three variables to desired values $(t_{x_2}, t_{z_2}, \sin\phi_2) = (0,0,0)$ can be completely solved with at least three outputs. However, it is also possible to find two equations to take two variables to their desired values and then a third one remains as a DOF. We propose to avoid the first case because defining more than two outputs generates a non-square system, in which, its non-invertibility makes difficult to prove stability of the control system.

Taking into account 1) the values of the tensor elements in the final location, 2) the solution of the homogeneous linear system that is generated when the outputs are equal to zero and 3) the invertibility of the matrix relating the output dynamics with the inputs, we can state:

- It is possible to design a square control system which can correct orientation and depth error, but it leaves the lateral error as a DOF. This lateral error cannot be corrected later considering the non-holonomic constraint of the robot. Thus, this case does not have practical interest.
- It is not possible to design a square control system which allows to correct orientation and lateral error, leaving the depth error as a DOF.
- It is feasible to design a square control system which can correct depth and lateral error, leaving the orientation as a DOF. The orientation error can be corrected in a second step considering that the robot uses a differential drive. We concentrate in exploiting this possibility.

III. 1D TT-BASED CONTROLLER DESIGN

We present the development of a two-steps control law, which firstly drives the robot to a desired position and then corrects its orientation. The first step is based on solving a tracking problem for a nonlinear system in order to correct x and z positions. The second step uses direct feedback from a tensor element to correct orientation.

A. First Step Controller - Position Correction

From now on let us define the initial location of the robot to be (x_1, z_1, ϕ_1), the target location $(x_3, z_3, \phi_3) = (0,0,0)$ and $(x_2(t), z_2(t), \phi_2(t))$ the current location, which varies as the robot moves. The goal is to drive the robot to the target location, this is, to reach $(x_2, z_2, \phi_2) = (0,0,0)$. The robot starts at the particular condition given in (4), and it should achieve the condition given in (5). The following sum of normalized tensor elements are selected as outputs

$$\begin{aligned} y_1 &= T_{112} + T_{121}, \\ y_2 &= T_{212} + T_{221}. \end{aligned} \tag{8}$$

We can see from (5) that these outputs go to zero as the robot moves to the target, and when $y_1 \equiv 0$, $y_2 \equiv 0$ the following linear system is given

$$\begin{bmatrix} T_{112}+T_{121} \\ T_{212}+T_{221} \end{bmatrix} = \begin{bmatrix} s\phi_1 & c\phi_1 \\ c\phi_1 & -s\phi_1 \end{bmatrix} \begin{bmatrix} t_{x_2} \\ t_{z_2} \end{bmatrix} = \begin{bmatrix} 0 \\ 0 \end{bmatrix}.$$

This system has unique solution $t_{x2} = 0$, $t_{z2} = 0$ for any value of ϕ_1 ($\det(\cdot) = -1$). Thus, it is accomplished $(t_{x2}, t_{z2}, \sin\phi_2) = (0,0,\sin\phi_2)$, which ensures position correction ($x_2 = 0$, $z_2 = 0$). To take the value of both outputs to zero in a smooth way we design a robust tracking controller. Let us define the tracking error as $e_1 = y_1 - y_1^d$, $e_2 = y_2 - y_2^d$. Thus, the error system is given as

$$\begin{bmatrix} \dot{e}_1 \\ \dot{e}_2 \end{bmatrix} = \begin{bmatrix} -\frac{c\phi_1}{T_N^m} & T_{122} - T_{111} \\ -\frac{s\phi_1}{T_N^m} & T_{222} - T_{211} \end{bmatrix} \begin{bmatrix} \upsilon \\ \omega \end{bmatrix} - \begin{bmatrix} \dot{y}_1^d \\ \dot{y}_2^d \end{bmatrix}. \tag{9}$$

This system has the form $\dot{\mathbf{e}} = \mathbf{M}(\mathbf{T}, \phi_1)\,\mathbf{u} - \dot{\mathbf{y}}^d$, where $\mathbf{M}(\mathbf{T}, \phi_1)$ corresponds to the decoupling matrix and $\dot{\mathbf{y}}^d$ represents a known disturbance. We need to invert the system in order to assign the desired dynamics using the inverse matrix

$$\mathbf{M}^{-1}(\mathbf{T}, \phi_1) = \frac{1}{\det(\mathbf{M})} \begin{bmatrix} T_{222} - T_{211} & T_{111} - T_{122} \\ \frac{s\phi_1}{T_N^m} & -\frac{c\phi_1}{T_N^m} \end{bmatrix} \tag{10}$$

where $\frac{1}{T_N^m}\left[(T_{122} - T_{111})\, s\phi_1 + (T_{211} - T_{222})\, c\phi_1\right] = \det(\mathbf{M})$ and $T_N^m = \sqrt{(T_{121}^m)^2 + (T_{212}^m)^2}$. At the final location $T_{221} = -t_{x1}$, $T_{212} = t_{x1}$, $T_{121} = t_{z1}$, $T_{112} = -t_{z1}$ and the other elements are zero. The proposed normalizing factor is never zero; however, $\det(\mathbf{M}) = 0$ at the final location. This entails the problem that the control inputs increase to infinite as the target is reached. We face this problem by switching to a bounded control law as is described later.

We treat the tracking problem as the stabilization of the error system in (9). We propose a robust control law to solve the tracking problem using sliding mode control [11], which has been already applied in visual control [4]. A common way to define sliding surfaces in an error system is directly to take the errors as sliding surfaces, in such a way that, if there exist switched feedback gains that make the states to evolve in $\mathbf{s} = 0$, then the tracking problem is solved.

$$\mathbf{s} = \begin{bmatrix} s_1 \\ s_2 \end{bmatrix} = \begin{bmatrix} e_1 \\ e_2 \end{bmatrix} = \begin{bmatrix} y_1 - y_1^d \\ y_2 - y_2^d \end{bmatrix}. \tag{11}$$

We use these sliding surfaces and the *equivalent control method* in order to find switched feedback gains to drive the state trajectory to $\mathbf{s} = 0$ and maintaining it there. From the equation $\dot{\mathbf{s}} = 0$, the so-called equivalent control is

$$\mathbf{u}_{eq} = \mathbf{M}^{-1}\dot{\mathbf{y}}^d. \tag{12}$$

A control law that ensures global stabilization of the error system has the form $\mathbf{u}_{sm} = \mathbf{u}_{eq} + \mathbf{u}_{disc}$, where $\mathbf{u}_{disc}$ is a two-dimensional vector containing switched feedback gains. We propose these gains as follows

$$\mathbf{u}_{disc} = \mathbf{M}^{-1} \begin{bmatrix} -k_1^{sm} sign(s_1) \\ -k_2^{sm} sign(s_2) \end{bmatrix} \tag{13}$$

where $k_1^{sm} > 0$ and $k_2^{sm} > 0$ are control gains. Although $\mathbf{u}_{sm}$ can achieve global stabilization of the error system, high gains may be needed, which can cause undesirable effects.

To alleviate this issue we add a pole placement term in the control law

$$\mathbf{u}_{pp} = \mathbf{M}^{-1} \begin{bmatrix} -k_1 & 0 \\ 0 & -k_2 \end{bmatrix} \begin{bmatrix} s_1 \\ s_2 \end{bmatrix} \tag{14}$$

where $k_1 > 0$ and $k_2 > 0$ are control gains. Finally, a decoupling-based control law that achieves robust global stabilization of the system (9) is as follows

$$\mathbf{u}_{db} = \begin{bmatrix} \upsilon_{db} \\ \omega_{db} \end{bmatrix} = \mathbf{u}_{eq} + \mathbf{u}_{disc} + \mathbf{u}_{pp} = \mathbf{M}^{-1} \begin{bmatrix} u_1 \\ u_2 \end{bmatrix} \tag{15}$$

where $u_1 = \dot{y}_1^d - k_1^{sm} sign\,(s_1) - k_1 s_1$, and $u_2 = \dot{y}_2^d - k_2^{sm} sign\,(s_2) - k_2 s_2$.

Note that this control law depends on the orientation of the fixed auxiliary camera. This orientation has to be computed only in the initial location and can be obtained from the epipoles that relates the initial and the target images. Any uncertainty in this orientation can be overcome by using the robust control law in (15). Moreover, a fix value can be used as is shown in Table I of the section V.

1) Solving the Singularity: The control law in (15) utilizes the decoupling matrix which presents a singularity problem for the final condition. We can note from (10) that the singularity affects to the computation of both velocities, however υ tends to zero as the robot reaches the target. To keep ω bounded and the outputs tracking their references, we propose to commute to a direct sliding mode controller when $\det(\mathbf{M})$ is near to zero. This kind of controller has been studied for output tracking through singularities [12] and has been applied previously [4]. For this case, the bounded sliding mode controller is as follows

$$\mathbf{u}_b = \begin{bmatrix} \upsilon_b \\ \omega_b \end{bmatrix} = \begin{bmatrix} M\ sign\,(s_1) \\ -N\ sign(s_2\ g(\mathbf{T})) \end{bmatrix} \tag{16}$$

where M and N are suitable gains, and $g(\mathbf{T})$ will be defined in the stability analysis (section IV). It is define by achieving the negativeness of a Lyapunov function derivative. The control law in (16) locally stabilizes the system (9) and is always bounded.

2) Desired Trajectories: The objective of tracking a reference is to take the outputs to zero in a smooth way and consequently, the robot performs a smooth motion in a desired time. We propose the following simple references

$$\begin{aligned} y_1^d &= \tfrac{T_{112}^{ini}+T_{121}^{ini}}{2}\left(1+\cos\left(\tfrac{\pi}{\tau}t\right)\right),\ 0 \le t \le \tau \\ y_1^d &= 0, \qquad\qquad\qquad\qquad\quad t > \tau \\ y_2^d &= \tfrac{T_{212}^{ini}+T_{221}^{ini}}{2}\left(1+\cos\left(\tfrac{\pi}{\tau}t\right)\right),\ 0 \le t \le \tau \\ y_2^d &= 0, \qquad\qquad\qquad\qquad\quad t > \tau \end{aligned} \tag{17}$$

where τ is the time to reach the target. Note that although initially the current image is the same than the starting one, there is enough information in the 1D trifocal tensor to have well defined references (see (4)).

B. Second Step Controller - Orientation correction

Once position correction have been reached ($t > \tau$), we can use any single tensor element whose dynamics depends on ω and its final value being zero. We select the dynamics $\dot{T}_{122} = -T_{112}\omega$. A suitable input ω that yields T_{122} exponentially stable is

$$\omega = k_\omega \tfrac{T_{122}}{T_{112}}, \qquad t > \tau \tag{18}$$

where $k_\omega > 0$ is a control gain. This angular velocity assigns the following dynamics to T_{122}, which is clearly exponentially stable

$$\dot{T}_{122} = -T_{112}\left(k_\omega \tfrac{T_{122}}{T_{112}}\right) = -k_\omega T_{122}. \tag{19}$$

Note that (18) never becomes singular because $T_{112} = -t_{z1}\cos\phi_2$ for $t = \tau$ and it tends to $T_{112} = -t_{z1} \neq 0$ as final value.

IV. STABILITY ANALYSIS

The first step controller is based on zeroing the defined outputs, so when these outputs reach to zero the so-called *zero dynamics* in the robot system is achieved. Zero dynamics is described by a subset of the state space which makes the output to be identically zero [13]. In the particular case of the robot system (2) with output vector (8), this set is given as follows

$$\begin{aligned} Z^* &= \left\{ \begin{bmatrix} x_2 & z_2 & \phi_2 \end{bmatrix}^T \mid y_1 \equiv 0,\ y_2 \equiv 0 \right\} \\ &= \left\{ \begin{bmatrix} 0 & 0 & \phi_2 \end{bmatrix}^T,\ \phi_2 \in \mathbb{R} \right\}. \end{aligned}$$

Zero dynamics in this control system means that when the chosen outputs are zero, the x and z-coordinates of the robot are corrected, but orientation may be different to zero. Then this zero dynamics yields $T_{122} = t_{z1}\sin\phi_2$, and therefore, when we make $T_{122} = 0$ then $\phi_2 = n\pi$ with $n \in \mathbb{Z}$, and the orientation is corrected. It is clear the exponential stability of T_{122} in the second step (19) for any $k_\omega > 0$ and we focus on proving stability for the tracking control law.

Proposition 1. A commuted control law that combines the decoupling-based control in (15) by switching to the bounded control in (16) whenever $|\det(\mathbf{M}(\mathbf{T}, \phi_1))| < T_h$, where T_h is a suitable threshold value, achieves global stabilization of the system in (9).

Proof: For a sliding mode controller we have to prove the existence of sliding modes. This means to develop a stability proof to know if the sliding surfaces can be reached in a finite time and the state trajectory can be maintained there. Let be the natural Lyapunov function for a sliding mode controller

$$V = V_1 + V_2,\ V_1 = \tfrac{1}{2}s_1^2,\ V_2 = \tfrac{1}{2}s_2^2 \tag{20}$$

which accomplish $V(s_1 = 0,\ s_2 = 0) = 0$ and $V > 0$ for all $s_1 \neq 0$, $s_2 \neq 0$.

$$\dot{V} = \dot{V}_1 + \dot{V}_2 = s_1\dot{s}_1 + s_2\dot{s}_2. \tag{21}$$

Let analyze each term of (21) for the decoupling based controller in (15). After some simple mathematical simplifications we have

$$\begin{aligned}\dot{V}_1 &= s_1\left(u_1-\dot{y}_1^d\right),\\ \dot{V}_1 &= s_1\left(\dot{y}_1^d-k_1^{sm}sign\left(s_1\right)-k_1s_1-\dot{y}_1^d\right),\\ \dot{V}_1 &= -k_1^{sm}\left|s_1\right|-k_1s_1^2.\end{aligned}$$

$$\begin{aligned}\dot{V}_2 &= s_2\left(u_2-\dot{y}_2^d\right),\\ \dot{V}_2 &= s_2\left(\dot{y}_2^d-k_2^{sm}sign\left(s_2\right)-k_2s_2-\dot{y}_2^d\right),\\ \dot{V}_2 &= -k_2^{sm}\left|s_2\right|-k_2s_2^2.\end{aligned}$$

$\dot{V}_1$ and $\dot{V}_2$ are negative definite (<0) iff the following inequalities are guaranteed for all $s_1\neq 0$, $s_2\neq 0$.

$$\begin{aligned}k_1^{sm} &> 0,\ k_1\geq 0,\\ k_2^{sm} &> 0,\ k_2\geq 0.\end{aligned}\tag{22}$$

Therefore, $\dot{V}<0$ iff both inequalities in (22) are fulfilled. Global convergence to the sliding surfaces can be achieved.

Now, let develop the existence conditions of sliding modes for the bounded controller (16). The same Lyapunov function in (20) is used, and for each term of (21) we have

$$\begin{aligned}\dot{V}_1 &= -\tfrac{M\cos\phi_1}{T_N^m}\left|s_1\right|\\ &\quad +s_1\left(\left(T_{122}-T_{111}\right)\left(-N\ sign(s_2\ g(\mathbf{T}))\right)-\dot{y}_1^d\right),\\ \dot{V}_2 &= s_2\left(-\tfrac{M\sin\phi_1}{T_N^m}\ sign\left(s_1\right)-\dot{y}_2^d\right)\\ &\quad -N\ \left|s_2\right|\ \left(T_{222}-T_{211}\right)sign\left(g(\mathbf{T})\right).\end{aligned}$$

Let be $A=-N\left(T_{122}-T_{111}\right)\ sign(s_2\ g(\mathbf{T}))-\dot{y}_1^d$ and $B=-\tfrac{M\sin\phi_1}{T_N^m}\ sign\left(s_1\right)-\dot{y}_2^d$. In order to enforce negativeness of $\dot{V}_2$ for some value of N, the function $g(\mathbf{T})$ have to be $g(\mathbf{T})=T_{222}-T_{211}$. Hence, we have

$$\begin{aligned}\dot{V}_1 &= -\tfrac{M\cos\phi_1}{T_N^m}\left|s_1\right|+s_1A,\\ \dot{V}_2 &= -N\ \left|s_2\right|\ \left|T_{222}-T_{211}\right|+s_2B.\end{aligned}$$

We can see that

$$\begin{aligned}\dot{V}_1 &\leq -\left(\tfrac{M\cos\phi_1}{T_N^m}-\left|A\right|\right)\left|s_1\right|,\\ \dot{V}_2 &\leq -\left(N\ \left|T_{222}-T_{211}\right|-\left|B\right|\right)\left|s_2\right|.\end{aligned}$$

$\dot{V}_1$ and $\dot{V}_2$ are negative definite (<0) iff the following inequalities are assured for all $s_1\neq 0$, $s_2\neq 0$.

$$\begin{aligned}N &> \tfrac{|B|}{|T_{222}-T_{211}|},\\ M &> \tfrac{T_N^m|A|}{\cos\phi_1}.\end{aligned}\tag{23}$$

Therefore, $\dot{V}<0$ iff both inequalities in (23) are fulfilled. The bounded controller does not need any information of system parameters and thus, its robustness is implicit.

According to the existence conditions of sliding modes, the bounded controller (16) is able to locally stabilize the system (9). Its attraction region is bigger as long as the control gains M and N are higher. Due to the bounded control law is also a switching one, the commutation from the decoupling-based to the bounded one does not affect stability of the control system. The first controller ensures entering to the attraction region of the second one. Once sliding surfaces are reached for any case of control law, the system's behavior is independent of matched uncertainties and disturbances [11]. Uncertainties in the system (9) due to ϕ_1 fulfill the matching condition, and as a result, robustness of the control system is accomplished. ■

V. SIMULATION RESULTS

In this section, we present some simulations of the overall control system as is established in the Proposition 1 for the first step and using (18) for the second one. Simulations have been performed in Matlab/Simulink. The results show how the main objective of driving the robot to a desired pose ((0,0,0^o) in all the cases) is attained regardless of reaching the singularity of the decoupling based control law, that is faced up by switching to the bounded control law. The 1D trifocal tensor is computed from metric information; however, it may be done using a five-matches method as in [9]. For the controllers, the time to reach the target position (τ) is fixed to 100 s, the threshold to switch to the bounded control (T_h) is fixed to 0.04, and control gains are set to $k_1=0.5$, $k_2=2$, $k_1^{sm}=0.02$, $k_2^{sm}=0.01$, $k_\omega=0.4$, $M=0.1$, $N=0.05$.

Fig. 2 shows the paths traced by the robot and the state variables evolution from four different initial locations. The thick solid line begins from (-8,-12,-33.69^o), the long dashed line from (-4,-14,-24^o), the solid line from (0,-10,0^o), and the short dashed line from (2,-19,-5^o). In the paths of Fig. 2(a) we can differentiate between three kind of autonomously performed robot motion. The solid lines correspond to a rectilinear motion to the target, while the long dashed line and the short dashed line both describe an inner curve and an outer curve before to reach the target respectively. The rectilinear motion is obtained when the initial rotation is such that $t_{x1}=t_{x2}=0$, which implies that the robot is pointing toward the target. The inner curve is generated when the initial rotation is such that $t_{x1}=t_{x2}>0$ and the outer curve when the initial rotation is such that $t_{x1}=t_{x2}<0$. In both later cases the robot performs autonomously an increase in rotation, which is efficiently corrected in the second step after 100 s, as can be seen in Fig. 2(b).

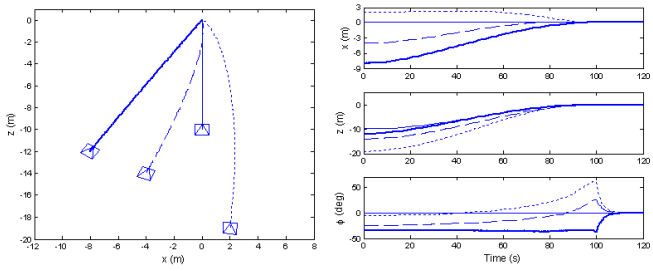

(a) (b)

Fig. 2. Resultant paths and state evolution (a) Paths on the $x-z$ plane. (b) State variables of the robot.

We can see in Fig. 3(a) that both outputs are driven to zero in 100 s for all the cases. This is achieved by using bounded inputs, which are presented in Fig. 3(b) for the case (-4,-14,-24^o). Both control inputs commute to a bounded value around 83 s due to the determinant of the decoupling matrix is less than the fixed threshold. We can also see how the angular velocity presents an exponential decay after 100 s, which takes the element T_{122} to reach zero as can be seen in Fig. 4. This forces the orientation to decrease with a fixed exponential rate, whose settling time is approximately 12.5 s ($5/k_\omega$).

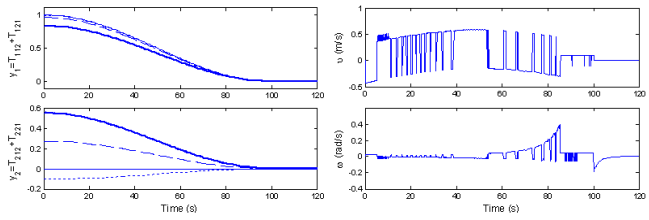

(a) (b)

Fig. 3. Outputs for the four cases and an example of inputs behavior. (a) Outputs. (b) Inputs for initial location (-4,-14,-24^o).

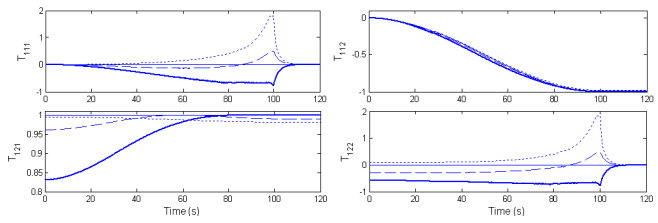

Fig. 4. Tensor elements evolution for $\mathbf{T}_1$.

TABLE I

FINAL LOCATION FOR THE PATHS IN FIG. 2.

	(-8,-12,-33.7) (m,m,^{o})	(-4,-14,-24) (m,m,^{o})	(0,-10,0) (m,m,^{o})	(2,-19,-5) (m,m,^{o})
Final locations considering the initial orientation ϕ as known.				
x (cm)	0.0299	0.7873	0	0.7525
z (cm)	0.0314	0.5758	-0.1454	1.6134
ϕ (^{o})	-0.7235	-1.1477	0	-0.3081
Final locations fixing $\phi = 0$ in the controller.				
x (cm)	0.0877	0.7041	0	0.5639
z (cm)	0.1032	0.7197	-0.1454	1.6887
ϕ (^{o})	-0.8248	-0.9436	0	0.0254

Table I shows that the target location is reached with good precision. The results in the first part of the table are obtained considering that the initial orientation ϕ_1 is known for each case. On the other hand, the second part of the table shows how the precision is preserved even if the initial orientation is fixed to $\phi_1 = 0$ in the controller for all the cases. We can assert that similar precision is obtained by fixing ϕ_1 in the range $-30 \leq \phi_1 \leq 30$, since that the sliding mode control law is robust against parametric uncertainty. For all the experiments, the mean squared tracking error is very low, in the order of 1×10^{-5}.

We can compute the trifocal tensor from omnidirectional cameras [9], so, we can assume that we have no restriction in the field of view, and consequently, the large rotation that the robot performs in the outer curve motion case can be carried out. Another option to keep the target in the field of view is to perform a initial rotation in order to reach the condition $t_{x1} = t_{x2} = 0$, and then, to execute the rectilinear motion to the target. This condition is easily detectable by checking $T_{221} = 0$ and $T_{222} = 0$.

A video showing the overall control system performance has been attached.

VI. CONCLUSIONS

In this paper we have presented a novel image-based approach to perform visual control for differential-drive robots using the elements of the 1D trifocal tensor directly in the control law. To the authors' knowledge, this is the first application of the 1D trifocal tensor in visual servoing. The visual control utilizes the usual teach-by showing strategy without requiring any a prior knowledge of the scene and does not need any auxiliary image. Our main contribution is that the proposed two-steps control law ensures total correction of lateral error, depth and orientation without necessity of switching to any other visual constraint rather than the 1D trifocal tensor. In the first step, we solve a tracking problem for a non-linear square system using sliding mode control. This provides robustness against matched uncertainties and disturbances. In the second step, a single tensor element is used to perform orientation correction. The effectiveness of our approach is tested via simulations.

REFERENCES

[1] P. Rives. Visual servoing based on epipolar geometry. In *IEEE/RSJ Int. Conf. on Intell. Robots and Systems*, pages 602–607, 2000.

[2] G. López-Nicolás, C. Sagüés, J.J. Guerrero, D. Kragic, and P. Jensfelt. Nonholonomic epipolar visual servoing. In *IEEE International Conference on Robotics and Automation*, pages 2378–2384, 2006.

[3] G. L. Mariottini, G. Oriolo, and D. Prattichizzo. Image-based visual servoing for nonholonomic mobile robots using epipolar geometry. *IEEE Transactions on Robotics*, 23(1):87–100, 2007.

[4] H. M. Becerra and C. Sagues. A sliding mode control law for epipolar visual servoing of differential-drive robots. In *IEEE/RSJ Int. Conf. on Intell. Robots and Systems*, pages 3058–3063, 2008.

[5] S. Benhimane and E. Malis. Homography-based 2D visual servoing. In *IEEE International Conference on Robotics and Automation*, pages 2397–2402, 2006.

[6] G. López-Nicolás, C. Sagüés, and J.J. Guerrero. Homography-based visual control of nonholonomic vehicles. In *IEEE International Conference on Robotics and Automation*, pages 1703–1708, 2007.

[7] R. I. Hartley and A. Zisserman. *Multiple View Geometry in Computer Vision*. Cambridge University Press, second edition, 2004.

[8] F. Dellaert and A. W. Stroupe. Linear 2D localization and mapping for single and multiple robot scenarios. In *IEEE International Conference on Robotics and Automation*, pages 688–694, 2002.

[9] J.J. Guerrero, A.C. Murillo, and C. Sagüés. Localization and matching using the planar trifocal tensor with bearing-only data. *IEEE Transactions on Robotics*, 24(2):494–501, 2008.

[10] G. López-Nicolás. *Visual Control of Mobile Robots Through Multiple View Geometry*. PhD thesis, DIIS, University of Zaragoza, Spain, June 2008.

[11] V. Utkin, J. Guldner, and J. Shi. *Sliding Mode Control in Electromechanical Systems*. CRC Press, Boca Raton, 1999.

[12] R. M Hirschorn. Output tracking through singularities. In *IEEE Conference on Decision and Control*, pages 3843–3848, 2002.

[13] S. Sastry. *Nonlinear Systems: Analysis, Stability and Control*. Springer, New York, 1999.